THE JOURNAL OF PHYSICAL CHEMISTRY B

ARTICLE

pubs.acs.org/JPCB

Cosolvent Preferential Molecular Interactions in Aqueous Solutions

M. Hamsa Priya,[†] H. S. Ashbaugh,[‡] and M. E. Paulaitis*[,†]

[†]William G. Lowrie Department of Chemical and Biomolecular Engineering, The Ohio State University, Columbus, Ohio 43210, United States

[‡]Department of Chemical and Biomolecular Engineering, Tulane University, New Orleans, Louisiana 70118, United States

Supporting Information

ABSTRACT: We extend the application of Kirkwood−Buff (KB) solution theory integrals to calculate cosolvent preferential interaction parameters from molecular simulations by deriving from a single simulation trajectory the excess chemical potential of the solute in addition to the solute−solvent molecular distribution functions. The solute excess chemical potential is derived from the potential distribution theorem (PDT) and used to define the local solvent domain around the solute, as distinguished from bulk solution. We show that this KB/PDT characterization of preferential molecular interactions resolves the problem of convergence of the preferential interaction parameter in the bulk solution limit, and as such, gives reliable estimates of preferential interaction parameters for methanol, ethanol, glycerol, and urea in aqueous cosolvent solutions with neopentane or tetramethyl ammonium ion as the solute. Preferential interaction parameters that are also calculated on the basis of cosolvent proximal distributions around the constituent methyl groups of the two solutes with the assumption of group additivity are in good agreement with those obtained by considering the molecular solute as a whole. The results suggest that this approach can be applied to estimate site-specific cosolvent preferential interaction parameters locally on the surface of complex, macromolecular solutes, such as proteins.

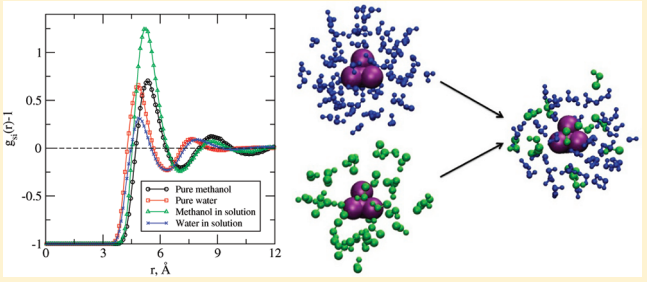

I. INTRODUCTION

Understanding cosolvent effects on protein solution thermodynamics is fundamental to many separation and purification processes in the pharmaceutical industry.[1−6] Cosolvents commonly used in these processes have diverse chemical functionalities and exhibit a wide range of solution behavior. Low molecular weight poly (ethylene glycol) and inorganic salts, such as $(NH_4)_2SO_4$, for example, are frequently used to induce protein crystallization,[3,7−12] while glycerol is often used to enhance crystal growth by reducing protein conformational flexibility.[3,13] Alcohols, on the other hand, can destabilize the native tertiary structure of proteins, leading to aggregation.[14,15]

On a molecular level, cosolvent effects on solutes in aqueous solutions are characterized in terms of preferential molecular interactions between the solute and cosolvent relative to solute−water interactions.[3,16] These molecular interactions can be inferred from macroscopic thermodynamic measurements; for example, equilibrium dialysis,[17] high precision densitometry,[18−20] and vapor pressure osmometry.[21] The so-called preferential interaction parameter derived from these measurements quantifies the change in solute chemical potential in response to adding cosolvent to the solution.

More recently, cosolvent preferential interactions have been studied using molecular simulations to obtain the cosolvent and water molecular distributions locally around the solute. The distribution functions are directly related to the cosolvent preferential interaction parameter through Kirkwood−Buff (KB) solution theory integrals, which characterize the local composition of the two-component solvent in the vicinity of the solute.[22−31]

For macromolecular solutes, such as proteins, the large number of cosolvent and water molecules solvating the protein allows the cosolvent preferential interaction parameter with the protein as a whole to be readily determined by simply counting cosolvent and water molecules in the local domain around the protein, and appropriately normalizing to bulk solution populations.[24,26,32] Cosolvent preferential interactions with the protein as a whole are, however, less informative than cosolvent preferential interactions with specific sites on the protein surface.

Site-specific preferential interactions, on the other hand, involve much fewer cosolvent and water molecules, and as such, are more sensitive to long-range oscillations in the KB integrals associated with the site-specific cosolvent and water molecular distribution functions. These long-range oscillations can be suppressed by "smearing" the distribution functions; that is, by using randomly selected reference points within a specified volume centered on individual water and cosolvent molecules to define their spatial locations with respect to the solute.[33−35]

Received: August 28, 2011
Revised: October 10, 2011
Published: October 12, 2011

Smearing facilitates the assessment of convergence of the KB integrals, leading to accurate partial molar volume calculations for molecular solutes with diverse chemical functionalities in water.[33−35] However, the convergence of partial molar compressibilities, evaluated as the difference between two KB integrals at different pressures, was found to be sensitive to the normalization of the cosolvent and water distribution functions,[34,36] suggesting that, even with smearing, properly normalizing the molecular distribution functions is essential for accurate calculations of site-specific preferential interaction parameters.

In this study, we extend the application of KB integrals with smearing to calculate cosolvent preferential interaction parameters for methanol, ethanol, glycerol, and urea in aqueous solution with a single molecular solute, neopentane or tetramethyl ammonium ion (TMA), chosen to represent prototypical hydrophobic and hydrophilic sites, respectively, on protein surfaces. We show that the preferential interaction parameter is sensitive to small variations in the cosolvent and water bulk solution densities required for normalizing the molecular distribution functions and fails to converge in the bulk solution limit when these small variations are not taken into account.

These small variations do not arise from statistical noise in the molecular distributions derived from the simulations, as previously suggested,[33] but are due to the preferential accumulation or depletion of cosolvent relative to water in the local domain around the solute, which naturally produces a countervailing depletion or accumulation of cosolvent relative to water in the bulk solution outside this local domain. The effect is observed even for large simulation box sizes, and is accounted for by computing effective bulk solution densities outside a well-defined local domain around each solute. We define this local domain based on a statistical thermodynamic description of preferential molecular interactions that focuses on the solute excess chemical potential, which is derived from molecular simulations using the potential distribution theorem (PDT).[37−39] The dual characterization of preferential interactions through KB solution theory and the PDT leads to the reliable convergence of the preferential interaction parameter, and as such, is central to our analysis of intermolecular preferential interactions for the systems considered.

II. THEORY

A. Preferential Interaction Parameters. Kirkwood−Buff (KB) solution theory[22,23] provides a statistical thermodynamic framework for evaluating the preferential interaction parameter, Γ_{sc}, from molecular distribution functions for the cosolvent (subscript c) and water (subscript w) around the solute (subscript s):

$$\Gamma_{sc} = \rho_c(G_{sc} - G_{sw}) \tag{1}$$

where ρ_c is the cosolvent number density in bulk aqueous solution. The KB integrals, G_{si}, are derived from $g_{si}(r|\mu VT)$, the solute/water and solute/cosolvent radial distribution functions evaluated in the grand canonical ensemble:

$$G_{si} = 4\pi \int_0^\infty (g_{si}(r|\mu VT) - 1)r^2\, dr \tag{2}$$

In practice, however, these integrals are evaluated from molecular simulations for closed systems at constant temperature and pressure or volume[27,28,40,41] by defining a local domain around the solute within the larger closed system. For the two solutes considered here, this local domain is reasonably taken to be a sphere of radius, R, centered on each solute; thus:

$$G_{si}(R) \approx 4\pi \int_0^R (g_{si}(r) - 1)r^2\, dr \tag{3}$$

The radial distribution function, $g_{si}(r)$, is evaluated in the closed simulation system from the density of component i within the local domain, $\rho_i(r < R) \equiv \rho_i g_{si}(r < R)$.

Normalization of $g_{si}(r)$ requires the bulk solution density, ρ_i, evaluated in the limit of $g_{si}(r > R) \rightarrow 1$. In principle, R corresponds to a radial distance beyond which $g_{si}(r > R) = 1$, allowing ρ_i to be obtained from the number density of component i outside the defined local domain around the solute:[33−36]

$$\rho_i = \frac{N_i - N_i(r \le R)}{V - 4\pi R^3/3} \tag{4}$$

where N_i is the total number of molecules of component i in the simulation, $N_i(r \le R)$ is the total number of molecules of component i in the defined local domain, and V is the volume of the simulation box. As shown below, however, even small deviations from $g_{si}(r > R) \rightarrow 1$ for the cosolvent and water species will be additive, rather than offsetting, in calculating the preferential interaction parameter from eq 1, and these small deviations lead to the divergence of Γ_{sc} as a function of increasing R. Further, resorting to larger simulations to obtain $g_{si}(r > R) \rightarrow 1$ for the two species is not a practical solution.

The local domain around the solute can also be specified by appealing to the thermodynamic definition of the preferential interaction parameter in terms of the change in the chemical potential of the solute, μ_s, in response to a change in cosolvent chemical potential, μ_c, at constant temperature, pressure, and solute concentration:[16,42,43]

$$\Gamma_{sc} = -\left(\frac{\partial \mu_s}{\partial \mu_c}\right)_{T,P,\rho_s} \tag{5}$$

or, equivalently, in terms of the partial derivative of the reduced excess chemical potential of the solute $\beta\mu_s^{ex}$ ($\equiv \mu_s^{ex}/k_BT$) with respect to the cosolvent number density:

$$\Gamma_{sc} = -\rho_c\left(\frac{\partial \beta\mu_s^{ex}}{\partial \rho_c}\right)\left[1 + \rho_c\left(\frac{\partial \beta\mu_c^{ex}}{\partial \rho_c}\right)\right]^{-1} \tag{6}$$

The subscripts stipulating that these partial derivatives are evaluated at constant T,P,ρ_s have been omitted to simplify the notation. We note that $(\partial\beta\mu_c^{ex}/\partial\rho_c)$, and therefore the factor in brackets, is independent of the definition of the local domain around the solute, which leads us to focus on the excess chemical potential of the solute and its cosolvent concentration dependence for this definition.

A statistical thermodynamic connection between the solute excess chemical potential and intermolecular interactions is given by the inverse form of the PDT:[37−39]

$$\beta\mu_s^{ex} = \ln \int_{-\infty}^{\infty} P(\varepsilon)e^{\beta\varepsilon}\, d\varepsilon \tag{7}$$

where ε is the solute−solvent (cosolvent and water) intermolecular interaction energy, $P(\varepsilon)$ is the probability distribution of these interaction energies, and the integral is evaluated over all possible solute−solvent configurations in the fully coupled system at constant temperature, $T = 1/k_B\beta$. Solute−solvent

intermolecular interactions can be partitioned into local interactions; that is, interactions within the local domain around the solute, and solute interactions with solvent molecules outside this domain.[37,38,44] Considering just those solute interactions with solvent molecules inside the local domain, defined above as a sphere of radius R centered on the solute, we can define a local excess chemical potential for the solute as

$$\beta\mu_s^{ex}(R) = \ln \int_{-\infty}^{\infty} P(\varepsilon|R) e^{\beta\varepsilon}\, d\varepsilon \quad (8)$$

where $P(\varepsilon|R)$ is the probability distribution of solute−solvent interaction energies for all solvent molecules within the radial distance R from the solute center. If the local domain is defined such that the solute interactions with all solvent molecules outside this domain are accurately described by a mean field, then solute−solvent preferential interactions are significant only within the local domain defined by R, which is identified as the radius beyond which $\mu_s^{ex}(R)$ computed from eq 8 is independent of R. We note that distinguishing local solute−solvent preferential interactions from nonlocal solute interactions with a mean field is valid if the probability distributions of solute−solvent interaction energies for all solvent molecules inside and outside the local domain are uncorrelated.[45,46]

B. Smeared Distribution Functions. Smearing the solvent (cosolvent or water) radial distribution functions to dampen long-range oscillations in the KB integrals takes advantage of the fact that the KB integrals are independent of the choice of the reference point that defines the spatial location of a solvent molecule relative to the solute. The chosen reference point may be a single point, such as the molecular center of mass, or uniformly distributed, for example, within a spherical volume of radius, λ, centered on the solvent molecule. The resulting density distribution is the average over density distributions derived from reference points taken from this distribution:

$$\rho(\vec{r};\lambda) = \frac{\int_{|\vec{r}'|<\lambda} \rho(\vec{r} + \vec{r}')\, d\vec{r}'}{4\pi\lambda^3/3} \quad (9)$$

The vector $\vec{r}'$ is defined relative to the solvent center at $\vec{r}$, and $\rho(\vec{r} + \vec{r}')$ is the local density at a distance $\vec{r} + \vec{r}'$ from the solute defined using $\vec{r}'$ as the reference point for that solvent molecule. The radial distribution of local densities is obtained by angle averaging over all solvent positions.

Smearing within a spherical volume around the molecular center of mass is sufficient for small cosolvent molecules, such as water and methanol, but results in the loss of information about the molecular conformations and orientational preferences of larger cosolvent molecules of practical interest; for example, ethanol, glycerol, and urea, where the functional groups comprising the cosolvent can interact with the solute in chemically distinct ways. For these cosolvents, smearing is carried out, as shown in Figure 1, by assigning uniform spherical distributions of reference points to each heavy atom j of a cosolvent molecule with m heavy atoms:

$$\rho(\vec{r};\{\lambda_j\}) = \frac{1}{m}\sum_{j=1}^{m} \frac{\int_{|\vec{r}'|<\lambda_j} \rho_j(\vec{r} + \vec{r}_j + \vec{r}')\, d\vec{r}'}{4\pi\lambda_j^3/3} \quad (10)$$

where $\vec{r}'$ is a reference point chosen randomly within radius λ_j of the heavy atom j, and $\vec{r}_j$ is the position vector of the heavy atom j relative to the solvent center $\vec{r}$. Because the shape of the cosolvent molecule is considered in this approach, the conformational flexibility of the cosolvent molecules and the orientational preferences of cosolvent molecules around the solute are implicitly taken into account.

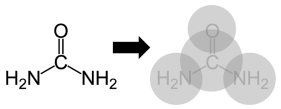

Figure 1. Concept of smearing the cosolvent distribution function: The location of a cosolvent molecule, in this case, urea, relative to the solute of interest is defined by a randomly selected reference point within the shaded spherical volumes centered on the different constituent groups of urea, rather than a single reference point, for example, the center of mass. Radii defining the spherical volumes for the different constituent groups are 2.3 Å for an oxygen atom (including TIP3P water) or hydroxyl group, 2.5 Å for a nitrogen atom or amine group, and 3.0 Å for a carbon atom or a methyl or methylene group. These radii are the radial distances up to which the oxygen−oxygen distribution function in pure water or the methanol oxygen−methanol oxygen proximal distribution function in 20 mol % methanol solution, the nitrogen−nitrogen proximal distribution function in 20 mol % urea solution, and the methyl−methyl proximal distribution function in 20 mol % methanol solution, respectively, equal zero.

C. Proximal Distribution Functions. The smeared solvent radial distribution functions described in the previous section are typically obtained by angle averaging the radial distributions of cosolvent and water densities over all positions around the solute. These radial distribution functions can also be evaluated by partitioning the space around the solute into subdomains corresponding to the solvent accessible constituent groups of the solute, and calculating proximal distribution functions within each subdomain.[35,47,48] The subdomain for each solvent molecule is determined by finding the minimum distance between the solvent molecule at $\vec{r}$ and the solute constituent group α at $\vec{r}_\alpha$. For a molecular solute consisting of n solvent accessible constituent groups:

$$|\vec{r} - \vec{r}_\alpha| - \sigma_\alpha = \min_{\beta=1,\ldots,n}|\vec{r} - \vec{r}_\beta| - \sigma_\beta \quad (11)$$

where σ_α is an effective excluded-volume radius for each group, $\alpha = 1,\ldots,n$. This radius is computed as the distance at which the corresponding proximal radial distribution function first equals unity, and accounts for size disparities among constituent groups of the solute. For neopentane and TMA, all four solvent accessible methyl groups on each solute are identical; therefore, $\sigma_\alpha = \sigma_\beta$ for all n for both solutes.

The cosolvent preferential interaction parameter within the subdomain for group α of the solute is

$$\Gamma_{sc,\alpha} = \rho_c(G_{sc,\alpha} - G_{sw,\alpha}) \quad (12)$$

where the corresponding KB integrals are

$$G_{si,\alpha}(R) = \int_0^R (g_{si,\alpha}(r) - 1)\frac{\partial V_\alpha(r)}{\partial r}\, dr \quad (13)$$

and each $g_{si,\alpha}(r)$ is integrated over the corresponding proximal volume, V_α.[47,48]

The cosolvent preferential interaction parameter for the entire solute is simply the sum of preferential interaction parameters computed for each subdomain:

$$\Gamma_{sc} = \sum_\alpha \Gamma_{sc,\alpha} \quad (14)$$

For solute groups that are completely inaccessible to the solvent, $\Gamma_{sc,\alpha} = 0$ in the sum.

III. MOLECULAR DYNAMICS SIMULATIONS

All simulations were performed for a single solute molecule (neopentane or TMA) in a periodic box of water and cosolvent (Table 1) using NAMD 2.6.[49] Each system was initially energy minimized by 10 000 steps of steepest descent minimization, and then equilibrated for 3 ns at 300 K and 1 bar. The average volume of the system, determined from the last 2 ns of this simulation, was used for the subsequent constant NVT simulation. Following further equilibration for 1 ns at constant NVT, configurations were saved every 0.05 ps over a 5 ns production run at constant NVT. Constant temperature was maintained by applying Langevin dynamics with a damping coefficient of 1 ps^{-1}. Pressure was held constant in the NPT simulations using a Nosé−Hoover Langevin piston[50,51] with a period of 200 fs and a decay of 100 fs. Electrostatic interactions were evaluated by particle-mesh Ewald summation[52] with a real-space cutoff of 12 Å. The same cutoff was applied to nonbonded dispersion interactions. The equations of motion were integrated with a 2 fs time step.

Water was modeled using the TIP3P potential[53] with the hydrogen−oxygen and hydrogen−hydrogen bond lengths held fixed using the SHAKE algorithm.[54] OPLS-united atom parameters for neopentane, TMA, methanol, and ethanol were taken from Jorgenson et al.,[55−57] as were the OPLS parameters for urea.[58] Glycerol was modeled using the all-atom CHARMM35 force field[59] with hydrogen atoms also constrained using the SHAKE algorithm.

Table 1. Number of Cosolvent and Water Molecules in the Simulation Systems as a Function of the Cosolvent Concentration[a]

cosolvent mole fraction	no. of cosolvent molecules	no. of water molecules
0.00	0	4138
0.05	205	3891
0.10	410	3686
0.20	820	3276
0.30	1229	2867
0.50	2048	2048
1.00	4096	0

[a] All simulations for cosolvents other than methanol were performed at a cosolvent mole fraction of 0.20.

IV. RESULTS AND DISCUSSION

The reduced solute excess chemical potential, $\beta\mu_s^{ex}$, is shown in Figure 2 as a function of the radius, R, of the spherical volume that defines the local domain around the solutes, neopentane and TMA, in aqueous solutions containing 20 mol % methanol, ethanol, glycerol, or urea as the cosolvent. In both cases, $\beta\mu_s^{ex}(R)$ initially decreases, becoming more negative with larger R, indicating an increasingly favorable solvation free energy as more solute−solvent interactions are included, before asymptotically approaching a limiting value for $R \geq 12$ Å for neopentane and $R \geq 8$ Å for TMA, independent of the cosolvent. The small variation observed beyond 9 Å observed for TMA in the 20 mol % aqueous methanol solution is less than the statistical uncertainty in the computed $\beta\mu_s^{ex}(R)$. Similar results are obtained for neopentane and TMA in aqueous solutions containing methanol as the cosolvent over a range of cosolvent concentrations from 5 to 50 mol % (Figure 8 in the Supporting Information).

The constant $\beta\mu_s^{ex}(R)$ beyond the specified value of R in each case indicates the lack of nonlocal preferential interactions with the solute in the sense that these long-range solute−solvent interactions effectively impose a mean field on the solute. The validity of this local model of solute−solvent (preferential) interactions is confirmed by plots of the joint probability distribution of local and nonlocal solute−solvent interaction energies, which show no correlation. Examples of these plots for neopentane and TMA in the 20 mol % aqueous methanol solution are given in the Supporting Information (Figure 9). Hence, we define the local domain around neopentane, where these preferential interactions are significant, as a spherical volume of radius, R = 12 Å, independent of the cosolvent, and we compute effective bulk solution densities for water and the

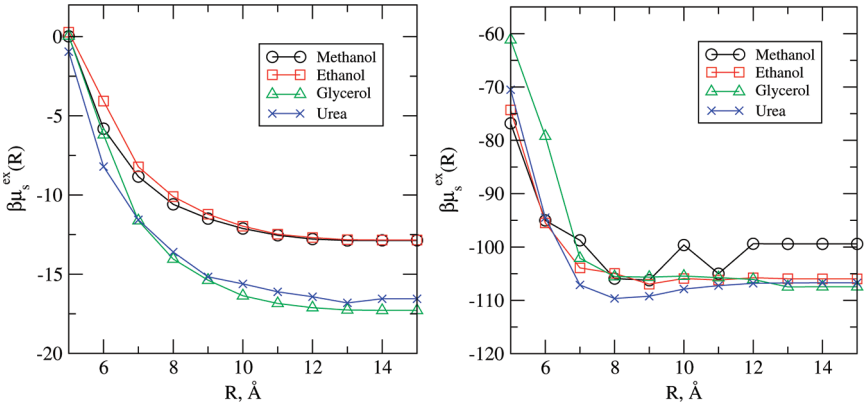

Figure 2. $\beta\mu_s^{ex}(R)$ for the solutes, neopentane (left panel) and TMA (right panel), in 20 mol % aqueous cosolvent solutions for different cosolvents: methanol (○), ethanol (red □), glycerol (green △), and urea (blue ×). Lines connecting the symbols are drawn to guide the eye. $\beta\mu_s^{ex}(R)$ is calculated from eq 8 by numerical integration. If the conditional probability distribution, $P(\varepsilon|R)$, in eq 8 is assumed to be a Gaussian distribution, the solute excess chemical potentials are ∼1 kcal/mol lower than the corresponding values obtained by numerical integration. The estimated uncertainties in $\mu_s^{ex}(R)$ are 0.152 kcal/mol at R = 5 Å and 0.237 kcal/mol at R = 14 Å, and correspond to the extent to which the high-energy tails of the conditional probability distribution in eq 8 are sampled for these two values of R.[60] Conditional probability distributions as a function of R for neopentane in the 20 mol % aqueous methanol solution are provided in the Supporting Information (Figure 7) as an example.

cosolvents as average densities over radial distances outside this local domain; that is, 12−15 Å from the center of neopentane. The local domain around TMA is likewise defined as a spherical volume of radius, R = 9 Å, independent of the cosolvent, and effective water and cosolvent bulk solution densities are computed as average densities over radial distances of 9−12 Å from the center of this solute.

The effects of smearing and normalization of the cosolvent and water radial distribution functions on the calculated $\Gamma_{sc}(R)$ are shown in Figure 3 for neopentane in a 20 mol % aqueous methanol solution. Smearing the radial distribution functions suppresses oscillations in $\Gamma_{sc}(R)$, while shifting the peaks to slightly greater radial distances. However, the convergence of $\Gamma_{sc}(R)$ depends to a much greater extent on the methanol and water bulk solution densities that are required for normalizing their respective radial distribution functions. When the bulk solution densities are evaluated using eq 4, $\Gamma_{sc}(R)$ begins to diverge at $R \approx 10$ Å, or roughly just beyond the second solvation shell (Figure 4). In contrast, convergence is obtained when effective bulk solution densities are evaluated as average methanol and water densities over radial distances of 12−15 Å from the solute. Average methanol and water densities calculated for any $R > 12$ Å and over solvent shells of widths from 3 to 9 Å up to a few angstroms from the sides of the simulation box were not significantly different (less than 0.1% variation).

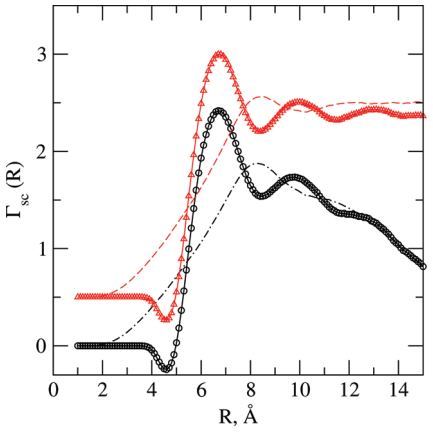

Figure 3. Preferential interaction parameter, $\Gamma_{sc}(R)$, as a function of the radius, R, of the local (spherical) domain around the solute for methanol (cosolvent) with neopentane (solute) in 20 mol % aqueous methanol solution. ○: $\Gamma_{sc}(R)$ computed by normalizing the radial distribution functions using eq 4. Red △: $\Gamma_{sc}(R)$ computed by normalizing the radial distribution functions using the average densities of methanol and water over radial distances of 12−15 Å from the center of neopentane. Solid lines through the symbols are drawn to guide the eye. The corresponding calculations using smeared radial distributions are shown as black dash-dotted, red dashed lines. For visual clarity, the latter results are shifted upward by 0.5 units.

This dependence on the effective bulk solution densities is examined in Figure 4 by comparing the neopentane−methanol and neopentane−water radial distribution functions, $g_{sc}(r)$ and $g_{sw}(r)$, respectively, for the solute in the aqueous cosolvent solution to the corresponding radial distribution functions for the solute in the two pure solvents. The peak positions of $g_{sc}(r)$ and $g_{sw}(r)$ in the left panel of Figure 4 are found to be essentially independent of whether methanol or water solvates neopentane as a pure solvent or in the aqueous solution. The primary peak heights of $g_{sc}(r)$ and $g_{sw}(r)$ for pure methanol and pure water are also nearly equivalent. There is a significant difference, however, in the primary peak heights for methanol and water in the aqueous solution. The primary peak for methanol is more than 4 times greater than that for water, which reflects the preferential accumulation of methanol relative to water in the local domain around neopentane.

This accumulation of methanol relative to water locally around the solute leads to the depletion of methanol relative to water for radial distances greater than 10 Å, as seen in the right panel of Figure 4. For pure water, $g_{sw}(r)$ converges to within ±0.01 of unity for $r > 10$ Å, and although oscillations in $g_{sc}(r)$ for pure methanol are longer ranged, convergence to within ±0.01 of unity is obtained for $r > 16$ Å. For the aqueous cosolvent solution, however, the deviations from unity persist with biases of $g_{sc}(r) < 1$ and $g_{sw}(r) > 1$ over the entire range of radial distances from 10 to 23 Å. The magnitudes of these deviations are small, on average less than ±1% of the overall methanol and water densities in the closed simulation system (Table 2). Even so, the distribution functions converge slowly, and the deviations are additive, rather than offsetting, in contributing to the preferential interaction parameter (eq 1), which leads to the divergence in $\Gamma_{sc}(R)$ observed in Figure 3.

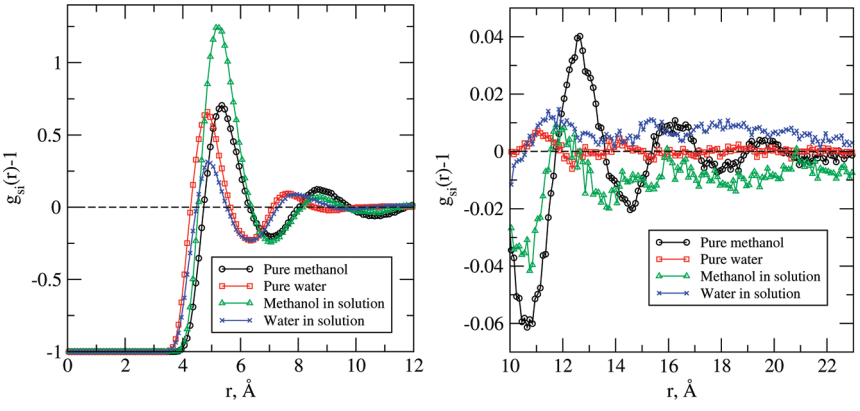

Figure 4. Left panel: Radial distribution functions, $g_{si}(r)$, for methanol (cosolvent) and water around neopentane (solute). Right panel: $g_{si}(r > 10$ Å) for methanol and water around neopentane. ○: Methanol distribution function in pure methanol. Red □: Water distribution function in pure water. Green △: Methanol distribution function in a 20 mol % aqueous methanol solution. Blue ×: Water distribution function in a 20 mol % aqueous methanol solution. Lines connecting the symbols are drawn to guide the eye.

dx.doi.org/10.1021/jp2083067 |J. Phys. Chem. B 2011, 115, 13633–13642

The behavior is intrinsic to solvent mixtures where differences in molecular sizes and the length scales of density fluctuations for the cosolvent and water are significant, and as such, place additional demands on normalization. It is also surprisingly long-ranged; the convergence of $\Gamma_{sc}(R)$ is obtained at $R \approx 12$ Å, or approximately two solvation shells of neopentane, and the entire simulation system considered encompasses more than four solvation shells of neopentane. Thus, resorting to larger simulations to calculate effective bulk solution densities from the total number of solvent molecules in the larger simulation box (eq 4) is not a practical solution.

Table 2. Effective Bulk Solution Densities for Methanol and Water in a 20 mol % Aqueous Methanol Solution, Defined by Their Average Number Densities over Radial Distances of 12 −15 Å from Neopentane (Solute), Compared to N_i/V, the Total Number of Solvent Molecules i in the Simulation Box Divided by the Volume of the Simulation Box[a]

species i	$\langle\rho_i(12 < r < 15\ \text{Å})\rangle$	N_i/V
methanol	5.3264	5.3769
water	21.5985	21.4810

[a] The partial molar volume of the solute at infinite dilution, $\overline{V}_s^{\infty} \ll V$, which can be neglected in these calculations. Densities are in units of molecules/nm^3.

Methanol preferential interaction parameters with neopentane and TMA in aqueous methanol solutions at different methanol concentrations are reported in Table 3. Smeared distribution functions for methanol and water are used in calculating Γ_{sc}, and the radial distribution functions are normalized using effective bulk solution densities computed, in each case, as the average water or methanol density over radial distances of 12−15 Å from the center of neopentane and 9−12 Å from the center of TMA. Figure 5 shows the convergence of $\Gamma_{sc}(R)$ for $R > 12$ Å (neopentane) and for $R > 9$ Å (TMA) over the entire range of methanol concentrations.

For neopentane in these aqueous methanol solutions, $\Gamma_{sc} > 0$, indicating the preferential accumulation of methanol relative to water in the local domain around the solute. In addition, Γ_{sc} increases by an order of magnitude with increasing methanol concentration from 5 to 50 mol %. Conversely, $\Gamma_{sc} < 0$ for TMA in the aqueous methanol solutions, indicating the preferential accumulation of water relative to methanol in the local domain around this solute, and Γ_{sc} becomes increasingly more negative over the same range of methanol concentration. The methanol concentration dependence of Γ_{sc} for both solutes cannot be attributed entirely to the change in the methanol density. As suggested by eq 6, nonideal solution thermodynamics can play a significant role primarily through the effect of methanol concentration on $(\partial\beta\mu_s^{ex}/\partial\rho_c)$, and to a lesser extent through the effect of methanol concentration on $(\partial\beta\mu_c^{ex}/\partial\rho_c)$.

Table 3. Preferential Interaction Parameters for Methanol (Cosolvent) with Solutes, Neopentane and TMA, in Aqueous Methanol Solutions at Different Methanol Concentrations[a]

	neopentane			TMA		
methanol mole fraction	ρ_c	Γ_{sc}	$\Sigma_\alpha\Gamma_{sc,\alpha}$	ρ_c	Γ_{sc}	$\Sigma_\alpha\Gamma_{sc,\alpha}$
0.05	1.5462	0.38 ± 0.16	0.41 ± 0.15	1.5476	−0.31 ± 0.05	−0.30 ± 0.08
0.10	2.9448	1.15 ± 0.29	1.17 ± 0.27	3.0380	−0.95 ± 0.17	−1.10 ± 0.25
0.20	5.3285	1.98 ± 0.22	1.89 ± 0.21	5.4124	−1.87 ± 0.14	−2.12 ± 0.23
0.30	7.3757	3.42 ± 0.34	3.29 ± 0.32	7.2590	−3.75 ± 0.12	−4.03 ± 0.20
0.50	10.1000	4.40 ± 0.43	4.33 ± 0.38	10.1899	−6.16 ± 0.51	−5.97 ± 0.48

[a] Γ_{sc} is evaluated by considering the molecular solute as a whole, and as the sum of preferential interaction parameters for the constituent groups of the solute (eq 14). Standard deviations are obtained by dividing the simulation trajectory into five equal parts and block averaging. Effective bulk solution densities for methanol, ρ_c, are computed as average densities over radial distances of 12−15 Å from the center of neopentane and over radial distances of 9−12 Å from the center of TMA. Densities are in units of molecules/nm^3.

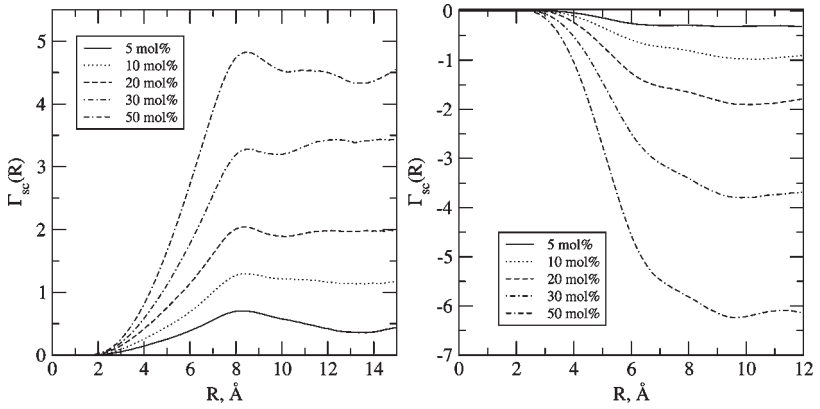

Figure 5. Preferential interaction parameters for methanol (cosolvent) with the solutes, neopentane (left panel) and TMA (right panel), in aqueous solutions at different methanol concentrations as a function of the radius, R, that defines the local domain around each solute. $\Gamma_{sc}(R)$ is calculated using smeared distribution functions for methanol and water. The distribution functions are normalized using effective bulk solution densities computed as average densities over radial distances of 12−15 Å from the center of neopentane and over radial distances of 9−12 Å from the center of TMA. Methanol mole fractions: 0.05, —; 0.10, · · ·; 0.20, — — —; 0.30, — · — ·—; 0.50, —— · —— · ——.

Also reported in Table 3 are methanol preferential interaction parameters with neopentane and TMA calculated as the sum of $\Gamma_{sc,\alpha}$ for the constituent methyl groups of the two solutes (eq 14). Smeared proximal distribution functions are used in these calculations. The agreement with Γ_{sc} evaluated for the molecular solutes as a whole is within statistical uncertainties of the calculations over the entire range of methanol concentrations. Although a more stringent test of group additivity would involve considering molecular solutes with heterogeneous constituent groups, the agreement obtained here suggests that proximal distribution functions can be useful for calculating cosolvent preferential interaction parameters with specific sites on the surface of a protein that are only partially solvent accessible.

Cosolvent preferential interaction parameters for methanol, ethanol, glycerol, and urea with neopentane and TMA in 20 mol % aqueous cosolvent solutions are reported in Table 4. Figure 6 shows the convergence of $\Gamma_{sc}(R)$ in each case. Cosolvent distribution functions used to calculate Γ_{sc} were smeared based on their constituent groups, and were normalized based on effective bulk solution densities computed as average densities over radial distances of 12−15 Å from the center of neopentane and 9−12 Å from the center of TMA.

Table 4. Cosolvent Preferential Interaction Parameters, Γ_{sc}, for Methanol, Ethanol, Glycerol, and Urea with Neopentane and TMA in 20 mol % Aqueous Cosolvent Solutions Evaluated by Smearing the Solvent Distribution Functions Based on the Constituent Groups of Each Cosolvent[a]

	solute, Γ_{sc}	
cosolvent	neopentane	TMA
methanol	1.98 ± 0.22	−1.87 ± 0.14
ethanol	8.99 ± 0.95	−3.27 ± 0.27
glycerol	−0.07 ± 0.69	−2.20 ± 0.48
urea	0.59 ± 0.58	−0.80 ± 0.28

[a] The distribution functions are normalized using effective bulk solution densities derived from average component densities over radial distances of 12−15 Å from the center of neopentane and 9−12 Å from the center of TMA.

From Table 4, $\Gamma_{sc} > 0$ for both alcohols with neopentane in the 20 mol % aqueous cosolvent solutions; further, Γ_{sc} for ethanol with neopentane is more than 4 times greater than that for methanol with this solute at the same cosolvent concentration. The much larger Γ_{sc} for ethanol relative to methanol is attributed to more favorable hydrophobic interactions with neopentane due to the additional methylene group. Conversely, $\Gamma_{sc} < 0$ for both alcohols with TMA in the 20 mol % aqueous cosolvent solutions, indicating that TMA is preferentially hydrated in the presence of either alcohol. In addition, the smaller difference in Γ_{sc} between ethanol and methanol for this solute as compared to neopentane implies that TMA preferentially interacts with the hydroxyl group of the alcohols. These observations suggest that ethanol, which is a protein precipitating agent as well as a denaturant, will preferentially interact with the hydrophobic sites on protein surfaces compared to the other common cosolvents in Table 4.

In contrast to these results for the alcohols, glycerol shows essentially no preferential interactions with neopentane — that is, $\Gamma_{sc} \approx 0$ (Table 4) — and the influence of this cosolvent on the preferential hydration of TMA is roughly the same as that for methanol. Urea preferential interactions with both solutes are much weaker than those for the alcohols, although $\Gamma_{sc} > 0$ for neopentane and $\Gamma_{sc} < 0$ for TMA, which is attributed to its high dipole moment (∼4 D) and small molecular volume.

An interesting distinction can be made between cosolvent effects characterized by Γ_{sc} in Table 4, and those manifested in $\beta\mu_s^{ex}(R)$ in Figure 2. Glycerol and urea exhibit almost no preferential interactions with neopentane as compared to the alcohols, and yet the local excess chemical potential for this hydrophobic solute is more favorable in the presence of glycerol or urea relative to either alcohol, which is counterintuitive. The differences emphasize that the preferential interaction parameter takes into account the bulk solution thermodynamics of the cosolvent in addition to cosolvent preferential interactions locally with the solute. The differences arise because of the greater thermodynamic cost to hydrating ethanol or methanol as compared to either glycerol or urea at the same concentration in aqueous solution, thus enhancing the partitioning of the alcohols into the local domain of the neopentane. The bulk solution thermodynamics of the cosolvent is not as significant for TMA because the solute−solvent (cosolvent and water) interactions dominate in this case.

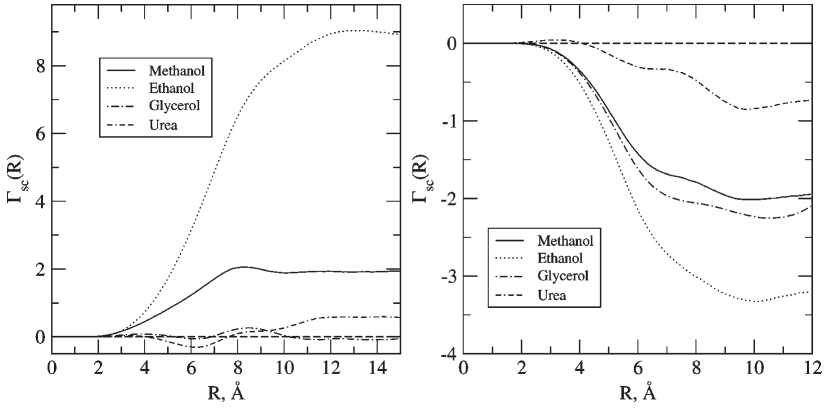

Figure 6. Cosolvent preferential interaction parameters, $\Gamma_{sc}(R)$, for methanol, ethanol, glycerol, and urea with neopentane (left panel) and TMA (right panel) in 20 mol % aqueous cosolvent solutions, evaluated using smeared solvent distribution functions. Cosolvent distribution functions were smeared based on their constituent groups. The distribution functions are normalized using effective bulk solution densities computed as average densities over radial distances of 12−15 Å from the center of neopentane and over radial distances of 9−12 Å from the center of TMA. —, methanol; · · ·, ethanol; — · — · —, glycerol; — — · — — · — —, urea.

dx.doi.org/10.1021/jp2083067 |J. Phys. Chem. B 2011, 115, 13633–13642

V. CONCLUSIONS

The preferential interaction parameter characterization of cosolvent effects accounts for all local solute−solvent (water and cosolvent) interactions, and as such, is sensitive to the definition of the local domain around the solute, as distinguished from bulk solution. We have shown that this sensitivity results from the dependence of the preferential interaction parameter on the definitions of cosolvent and water bulk solution densities when Γ_{sc} is computed from molecular distribution functions (eq 1). If small variations in the bulk solution densities are not taken into account, Γ_{sc} fails to converge in the bulk solution limit.

This convergence problem is resolved here by deriving from a single molecular simulation trajectory the excess chemical potential of the solute in addition to the solute−solvent molecular distribution functions. The solute excess chemical potential is used to distinguish local solute−solvent interactions from nonlocal interactions, and thereby defines the local domain around the solute. Effective bulk solution densities for the cosolvent and water are then computed as average densities outside this well-defined local domain, and the preferential interaction parameter derived from the molecular distribution functions within the local domain, normalized by these average densities. Incorporating the solute excess chemical potential as described here takes advantage of relying on intermolecular interactions, rather than longer range intermolecular positional correlations, to define the local domain around the solute. The molecular thermodynamic details of the relationship between solute−solvent intermolecular interactions and the solute excess chemical potential that can be derived from molecular simulations are also likely to offer physical insights into preferential molecular interactions that cannot be obtained by considering molecular distribution functions alone. Of course, Γ_{sc} can be computed directly from the solute excess chemical potential evaluated as a function of the cosolvent composition (eq 6). This approach is the subject of a forthcoming publication.

In applying this approach to calculate preferential interaction parameters for methanol, ethanol, glycerol, and urea in aqueous cosolvent solutions with neopentane or TMA as the solute, we demonstrated that convergence is achieved, and as a consequence, reliable estimates of Γ_{sc} are obtained in all cases. Moreover, we obtained a significantly smaller local domain for the hydrophilic solute compared to that for the hydrophobic solute, but, more importantly, the local domain is essentially independent of the different cosolvents considered in both cases. The finding leads us to conclude that this approach may be straightforwardly applied to a wide variety of chemically diverse solutes in aqueous solutions with these common cosolvents. Our implementation of smearing the molecular distribution functions based on the constituent heavy atoms of the molecular cosolvents also facilitates extending this approach to other cosolvents.

The preferential interaction parameter characterization of cosolvent effects for neopentane in aqueous solution shows that this hydrophobic solute is preferentially solvated by methanol, and to a much greater extent by ethanol, but the solute exhibits almost no preference for glycerol or urea over water. In contrast, TMA is preferentially hydrated in the presence of all four cosolvents, although to a lesser extent for urea compared to the other three cosolvents. Interestingly, urea exhibits almost no preferential interactions with either the hydrophobic solute or the hydrophilic solute in aqueous solution.

Finally, preferential interaction parameters calculated for methanol with neopentane and TMA as the sum of cosolvent preferential interaction parameters for the individual methyl groups of these solutes are found to be in excellent agreement with those obtained by considering each solute molecule as a whole. Although group additivity is not expected to hold in general for complex, chemically heterogeneous solutes, our results support the application and further assessment of proximal distribution functions with the assumption of group additivity to estimate cosolvent preferential interaction parameters for larger, more complex solute molecules. An interesting application of this approach would be to evaluate preferential interaction parameters locally across the surface of a protein, in essence to obtain a cosolvent preferential interaction map of the protein surface.

■ ASSOCIATED CONTENT

Supporting Information. Additional figures. This material is available free of charge via the Internet at http://pubs.acs.org.

■ AUTHOR INFORMATION

Corresponding Author
*E-mail: paulaitis.1@osu.edu.

■ ACKNOWLEDGMENT

Financial support from the National Science Foundation (MEP: BES-0555281; HSA: CTS-07469555) and the Department of Energy (DE-FG02-04ER25626) is gratefully acknowledged. We also thank Dilip Asthagiri (Johns Hopkins) for his insightful comments on the work.

■ REFERENCES

(1) Gould, P. L.; Goodman, M.; Hanson, P. A. Investigation of the solubility relationships of polar, semi-polar and non-polar drugs in mixed co-solvent systems. *Int. J. Pharm.* **1984**, *19*, 149–159.

(2) Ruelle, P.; Kesselring, U. W. The hydrophobic effect. 1. A consequence of the mobile order in H-bonded liquids. *J. Pharm. Sci.* **1998**, *87*, 987–997.

(3) Timasheff, S. N. Control of protein stability and reactions by weakly interacting cosolvents: The simplicity of the complicated. *Adv. Protein Chem.* **1998**, *51*, 355–432.

(4) Ruckenstein, E.; Shulgin, I. L. Solubility of drugs in aqueous solutions: Part 1. Ideal mixed solvent approximation. *Int. J. Pharm.* **2003**, *258*, 193–201.

(5) Ruckenstein, E.; Shulgin, I. L. Solubility of drugs in aqueous solutions: Part 2: Binary nonideal mixed solvent. *Int. J. Pharm.* **2003**, *260*, 283–291.

(6) Baynes, B. M.; Trout, B. L. Rational design of solution additives for the prevention of protein aggregation. *Biophys. J.* **2004**, *87*, 1631–1639.

(7) Retailleau, P.; Ducruix, A.; Riès-Kautt, M. Importance of the nature of anions in lysozyme crystallization correlated with protein net charge variation. *Acta Crystallogr., Sect. D* **2002**, *58*, 1576–1581.

(8) Velev, O. D.; Kaler, E. W.; Lenhoff, A. M. Protein interactions in solution characterized by light and neutron scattering: Comparison of lysozyme and chymotrypsinogen. *Biophys. J.* **1998**, *75*, 2682–2697.

(9) Cheng, Y.; Lobo, R. F.; Sandler, S. I.; Lenhoff, A. M. Kinetics and equilibria of lysozyme precipitation and crystallization in concentrated ammonium sulfate solutions. *Biotechnol. Bioeng.* **2006**, *94*, 177–188.

(10) McPherson, A. *Crystallization of Biological Macromolecules*; Cold Spring Harbour Laboratory Press: New York, 1999.

(11) McPherson, A. Crystallization of proteins from polyethylene glycol. *J. Biol. Chem.* **1976**, *251*, 6300–6303.
(12) Gilliland, G. L.; Tung, M.; Blakeslee, D. M.; Ladner, J. E. Biological macromolecule crystallization database, version 3.0: New features, data and the NASA archive for protein crystal growth data. *Acta Crystallogr., Sect. D* **1994**, *50*, 408–413.
(13) Sousa, R. Use of glycerol, polyols and other protein structure stabilizing agents in protein crystallization. *Acta Crystallogr., Sect. D* **1995**, *51*, 271–277.
(14) Ikeda, K.; Hamaguchi, K. Interaction of alcohols with lysozyme I. Studies on circular dichroism. *J. Biochem.* **1970**, *68*, 785–794.
(15) Liu, W.; Bratko, D.; Prausnitz, J. M.; Blanch, H. W. Effect of alcohols on aqueous lysozyme-lysozyme interactions from static light scattering measurements. *Biophys. Chem.* **2004**, *107*, 289–298.
(16) Casassa, E. F.; Eisenberg, H. Thermodynamic analysis of multicomponent solutions. *Adv. Protein Chem.* **1964**, *19*, 287–395.
(17) Scatchard, G. Physical chemistry of protein solutions. I. Derivation of the equations for the osmotic pressure. *J. Am. Chem. Soc.* **1946**, *68*, 2315–2319.
(18) Lee, J. C.; Timasheff, S. N. The stabilization of proteins by sucrose. *J. Biol. Chem.* **1981**, *256*, 7193–7201.
(19) Gekko, K.; Timasheff, S. N. Mechanism of protein stabilization by glycerol: Preferential hydration in glycerol-water mixtures. *Biochemistry* **1981**, *20*, 4667–4676.
(20) Arakawa, T.; Timasheff, S. N. Preferential interactions of proteins with salts in concentrated solutions. *Biochemistry* **1982**, *21*, 6545–6552.
(21) Courtenay, E. S.; Capp, M. W.; Anderson, C. F.; Record, M. T., Jr. Vapor pressure osmometry studies of osmolyte−protein interactions: Implications for the action of osmoprotectants in vivo and for the interpretation of "osmotic stress" experiments in vitro. *Biochemistry* **2000**, *39*, 4455–4471.
(22) Kirkwood, J. G.; Buff, F. P. The statistical mechanical theory of solutions. I. *J. Chem. Phys.* **1951**, *19*, 774–777.
(23) Smith., P. E. Chemical potential derivatives and preferential interaction parameters in biological systems from Kirkwood−Buff theory. *Biophys. J.* **2006**, *91*, 849–856.
(24) Baynes, B. M.; Trout, B. L. Proteins in mixed solvents: A molecular-level perspective. *J. Phys. Chem. B* **2003**, *107*, 14058–14067.
(25) Kang, M.; Smith, P. E. Preferential interaction parameters in biological systems by Kirkwood−Buff Theory and computer simulation. *Fluid Phase Equilib.* **2007**, *256*, 14–19.
(26) Shukla, D.; Shinde, C.; Trout, B. L. Molecular computations of preferential interaction coefficients of proteins. *J. Phys. Chem. B* **2009**, *113*, 12546–12554.
(27) Shah, P. P.; Roberts, C. J. Molecular solvation in water-methanol and water-sorbitol mixtures: The roles of preferential hydration, hydrophobicity, and the equation of state. *J. Phys. Chem. B* **2007**, *111*, 4467–4476.
(28) Smith, P. E. Computer simulation of cosolvent effects on hydrophobic hydration. *J. Phys. Chem. B* **1999**, *103*, 525–534.
(29) Smith., P. E. Cosolvent interactions with biomolecules: Relating computer simulation data to experimental thermodynamic data. *J. Phys. Chem. B* **2004**, *108*, 18716–18724.
(30) Ghosh, T.; Kalra, A.; Garde, S. On the salt-induced stabilization of pair and many-body hydrophobic interactions. *J. Phys. Chem. B* **2005**, *109*, 642–651.
(31) Athawale, M. V.; Dordick, J. S.; Garde, S. Osmolyte trimethylamine-N-oxide does not affect the strength of hydrophobic interactions: Origin of osmolyte compatibility. *Biophys. J.* **2005**, *89*, 858–866.
(32) Smolin, N.; Winter, R. Effect of temperature, pressure, and cosolvents on structural and dynamic properties of the hydration shell of SNase: A molecular dynamics computer simulation study. *J. Phys. Chem. B* **2008**, *112*, 997–1006.
(33) Lockwood, D. M.; Rossky, P. J. Evaluation of functional group contribution to excess volumetric properties of solvated molecules. *J. Phys. Chem. B* **1999**, *103*, 1982–1990.
(34) Lockwood, D. M.; Rossky, P. J.; Levy, R. M. Functional group contributions to partial molar compressibilities of alcohols in water. *J. Phys. Chem. B* **2000**, *104*, 4210–4217.
(35) Sangwai, A. V.; Ashbaugh, H. S. Aqueous partial molar volumes from simulation and individual group contributions. *Ind. Eng. Chem. Res.* **2008**, *47*, 5169–5174.
(36) Matubayasi, N.; Levy, R. M. Thermodynamics of the hydration shell. 2. Excess volume and compressibility of a hydrophobic solute. *J. Phys. Chem.* **1996**, *100*, 2681–2688.
(37) Beck, T. L.; Paulaitis, M. E.; Pratt, L. R. *The Potential Distribution Theorem and Models of Molecular Solutions*; Cambridge University Press: Cambridge, 2006.
(38) Pratt, L. R.; Asthagiri, D. Potential distribution methods and free energy models of molecular solutions. In *Free Energy Calculations: Theory and Applications in Chemistry and Biology, Vol. 86 of Springer Series in Chemical Physics*; Chipot, C., Pohorille, A., Eds.; Springer: New York, 2007; Chapter 9, pp 323−351.
(39) Widom, B. Potential-distribution theory and the statistical mechanics of fluids. *J. Phys. Chem.* **1982**, *86*, 869–872.
(40) Chitra, R.; Smith, P. E. Preferential interactions of cosolvents with hydrophobic solutes. *J. Phys. Chem. B* **2001**, *105*, 11513–11522.
(41) Kokubo, H.; Pettitt, B. M. Preferential solvation in urea solutions at different concentrations: Properties from simulation studies. *J. Phys. Chem. B* **2007**, *111*, 5233–5242.
(42) Timasheff, S. N. Protein solvent preferential interactions, protein hydration, and the modulation of biochemical reactions by solvent components. *Proc. Natl. Acad. Sci. U.S.A.* **2002**, *99*, 9721–9726.
(43) Schellman, J. A. Selective binding and solvent denaturation. *Biopolymers* **1987**, *26*, 549–559.
(44) Paulaitis, M. E.; Pratt, L. R. Hydration theory for molecular biophysics. *Adv. Protein Chem.* **2002**, *62*, 283–310.
(45) Dixit, P. D.; Merchant, S.; Asthagiri, D. Ion selectivity in the KcsA potassium channel from the perspecitve of the ion binding site. *Biophys. J.* **2010**, *96*, 2138–2145.
(46) Dixit, P. D.; Asthagiri, D. The role of bulk protein in local models of ion-binding to proteins: Comparative study of KcsA, its semisynthetic analog with a locked-in binding site, and valinomycin. *Biophys. J.* **2011**, *100*, 1542–1549.
(47) Ashbaugh, H. S.; Paulaitis, M. E. Effect of solute size and solute−water attractive interactions on hydration water structure around hydrophobic solutes. *J. Am. Chem. Soc.* **2001**, *123*, 10721–10728.
(48) Ashbaugh, H. S.; Paulaitis, M. E. Monomer hydrophobicity as a mechanism for the LCST behavior of poly(ethylene oxide) in water. *Ind. Eng. Chem. Res.* **2006**, *45*, 5531–5537.
(49) Kalé, L.; Skeel, R.; Bhandarkar, M.; Brunner, R.; Gursoy, A.; Kraweta, N.; Phillips, J.; Shinozaki, A.; Varadarajan, K.; Schulten, K. NAMD2: Greater scalability for parallel molecular dynamics. *J. Comput. Phys.* **1999**, *151*, 283–312.
(50) Martyna, G. J.; Tobias, D. J.; Klein, M. L. Constant pressure molecular dynamics algorithms. *J. Chem. Phys.* **1994**, *101*, 4177–4189.
(51) Feller, S. E.; Zhang, Y.; Pastor, R. W.; Brooks, B. R. Constant pressure molecular dynamics simulations: The langevin piston method. *J. Chem. Phys.* **1995**, *103*, 4613–4621.
(52) Darden, T.; York, D.; Pedersen, L. Particle mesh ewald: An N log(N) method for ewald sums in large systems. *J. Chem. Phys.* **1993**, *98*, 10089–10092.
(53) Jorgensen, W. L.; Chandrasekhar, J.; Madura, J. D.; Impey, R. W.; Klein, M. L. Comparison of simple potential functions for simulating liquid water. *J. Chem. Phys.* **1983**, *79*, 926–935.
(54) Ryckaert, J. P.; Ciccotti, G.; Berendsen, H. J. C. Numerical integration of the cartesian equations of motion of a system with constraints: Molecular dynamics of n-alkanes. *J. Comput. Phys.* **1977**, *23*, 327–341.
(55) Jorgensen, W. L.; Madura, J. D.; Swenson, C. J. Optimized intermolecular potential functions for liquid hydrocarbons. *J. Am. Chem. Soc.* **1984**, *106*, 6638–6646.

(56) Jorgensen, W. L.; Gao, J. Monte Carlo simulations of the hydraion of ammonium and carboxylate ions. *J. Phys. Chem.* **1986**, *90*, 2174–2182.

(57) Jorgensen, W. L. Optimized intermolecular potential function for liquid alcohols. *J. Phys. Chem.* **1986**, *90*, 1276–1284.

(58) Duffy, E. M.; Severance, D. L.; Jorgensen, W. L. Urea: Potential functions, log P, and free energy of hydration. *Isr. J. Chem.* **1993**, *33*, 323–330.

(59) Kamath, G.; Guvench, O.; MacKerell, A. D., Jr. CHARMM additive all-atom force field for acyclic carbhohydrates and inositol. *J. Chem. Theory Comput.* **2008**, *4*, 765–778.

(60) Utiramerur, S.; Paulaitis, M. E. Cooperative hydrophobic/hydrophilic interactions in the hydration of dimethyl ether. *J. Chem. Phys.* **2010**, *132*, 155102–9.